Carbohydrate Polymers 84 (2011) 990–996

Contents lists available at ScienceDirect

Carbohydrate Polymers

journal homepage: www.elsevier.com/locate/carbpol

The mineralization of electrospun chitosan/poly(vinyl alcohol) nanofibrous membranes

Dongzhi Yang[a,*], Kun Yu[a], Yufei Ai[a], Hongpeng Zhen[a], Jun Nie[a], John F. Kennedy[b]

[a] Key Laboratory of Carbon Fiber and Functional Polymers, Ministry of Education, State Key Laboratory of Chemical Resource Engineering, Beijing University of Chemical Technology, Beijing 100029, China
[b] Chembiotech Laboratories, University of Birmingham Research Park, Vincent Drive, Birmingham B15 2SQ, UK

ARTICLE INFO

Article history:
Received 29 November 2010
Received in revised form
15 December 2010
Accepted 16 December 2010
Available online 28 December 2010

Keywords:
Mineralization
Chitosan
Electrospinning
Calcium carbonate

ABSTRACT

Based on the principles of biomineralization, a calcium carbonate ($CaCO_3$) and chitosan composite membrane was prepared by mineralized of calcium carbonate on chitosan/poly(vinyl alcohol) nanofibers under dynamic condition. The morphology and structure of membranes were characterized by scanning electron microscopy, X-ray diffraction and Fourier transform infrared spectroscopy. The results showed that the chitosan/poly(vinyl alcohol) nanofibers produced thin $CaCO_3$ island crystals, which interlaced with the chitosan fiber not only on the surface of the membrane but also within the membrane. The crystals could develop into a continuous $CaCO_3$ membrane on the fibers at latter stage of mineralization, the obtained crystals was mainly calcite type of $CaCO_3$, and with small quantity of vaterite. MTT test and SEM imaging indicated that the attachment and growth of mouse fibroblast were well on the surface of $CaCO_3$/chitosan/PVA composite membrane, and this composite has a good application prospect in the field of biomedical materials.

1. Introduction

As well known, biomineral materials, such as teeth, bones and shells, are composed of inorganic crystals and biopolymers. In the process of biomineralization, the growth of inorganic crystals is determined in a way by organic substrates. The biominerals formed manifest unique structures and special properties compared with their inorganic counterparts (Egan, Mavuso, & Ncokazi, 2001; Grassmann, Muller, & Lobmann 2002; Mann, 2001). In contrast to conventional chemical synthesis by covalent bond interaction, biomineralization is a process of molecular-recognition and molecular self-assemble through weaker interactions between molecules. Potential application of biomimetic coatings covered a broad range of industries and medicine (He et al., 2005; Rhoads, Beyenal, Lewandowski, & Environ, 2005; Zhang, Wang, Gu, Hartmann, & Mohwald, 2005).

The bone regeneration is a typical biomineral process, it had been noticed that the biomimetic organoapatite materials had broad applications for bone tissue engineering (Gao, He, Chen, & Yi, 2003; Osamu, 2005; Storrie & Stupp, 2005; Zhang et al., 2003). The highly porous biodegradable 3D-scaffolds for adhesion of cells and signaling molecules, having interconnected pore network structure was very important for tissue engineering. Meanwhile, studies indicate that a favourable pore size and micro-structural composition are important factors facilitating in-growth of fibrovascular tissue or bone from the host. A various techniques to generate porous scaffolds for tissue engineering have been reported, however, the scaffolds prepared by these techniques cannot be easily adjusted to provide nanoscale features as present in the natural extra-cellular matrix. The structures generated by electrospinning contain nanoscale fibers with microscale interconnected spaces, resembling the topographic features of the ECM (Doshi & Reneker, 1995; Reneker & Chun, 1996).

Being a biocompatible, biodegradable and bioactive material, chitosan in the form of membranes offers a great potential as a substrate in mineralization processes in vitro (Ehrlich et al., 2006; Gooday, Prosser, illman, & Cross, 1991; Hirano, Inui, & Yamamoto, 1995; Hirano, Yamamoto, & Inui, 1997; Ho et al., 2005; Liang, Zhao, Shen, Wang, & Xu, 2004; Muzzarelli, 2009, 2011; Neira-Carrillo et al., 2005), as well as tissue engineering scaffold. However, because of the poor electrospinnability and high brittleness of chitosan, we employed chitosan and few of PVA together as a complex organic matrix.

This new biomineralization organic matrix might have potential for making new artificial bone materials. So study the mineralization of hydroxyapatite, the principal mineral of bone, was very necessary. In our recent work (Yang et al., 2008), a mineralization biocomposite of hydroxyapatite (HAp) was prepared by using N-carboxyethyl chitosan/PVA electrospun membranes as organic matrix, and HAp was formed in supersaturated $CaCl_2$ and KH_2PO_4

* Corresponding author. Tel.: +86 010 64421310; fax: +86 010 64421310.
E-mail address: yangdz@mail.buct.edu.cn (D. Yang).

0144-8617/$ – see front matter © 2011 Published by Elsevier Ltd.
doi:10.1016/j.carbpol.2010.12.057

solution. The influences of carboxylic acid groups in N-carboxyethyl chitosan/PVA fibrous scaffold and polyanionic additive poly(acrylic acid) (PAA) in the incubation solution on the crystal distribution of the HAp were investigated. In the above study, after the mineral membrane was taken out from the incubation solution, it must be treated with alkaline sodium hydroxide solution in order to obtain HAp. Otherwise phosphate was formed, rather than HAp.

In addition, calcium carbonate has been recognized as bone filling material and its good osteoconductivity had been appreciated in recent studies (Piattelli, Podda, & Scarano, 1997; Walsh et al., 2003). Coral mineral (calcite or aragonite forms of calcium carbonate, 99%) has had considerable success considering its porous structure (which ranges from 150 to 500 μm) is similar to cancellous bone and is one of a limited number of materials that will form chemical bonds with bone and soft tissues in vivo (Nissan, 2003).

Although the biomineralization and crystallization processes associated with $CaCO_3$ have been extensively studied, up to now, electrospinning membrane used to mimic organoapatite matrix has been seldom reported, is very interesting to biomedical material.

The present study is to develop calcium rich yet mechanically stable chitosan/$CaCO_3$ composite nanofibrous membranes to simulate coral structure, and how it might nucleate calcium carbonate.

2. Experimental

2.1. Materials

Chitosan (Mw 100,000, degree of deacetylation 85%) was obtained from Zhejiang Golden-Shell Biochemical Co. (Zhejiang, China). Polyvinyl alcohol (PVA, degree of polymerization 3500, 88% hydrolyzed) was obtained from Kuraray Co. (Takyo, Japan). All other reagents were obtained from Beijing Chemical Agent Co. (Beijing, China).

2.2. Electrospinning process of composite nanofibrous membrane

A 7 wt% of chitosan solution was made by dissolution of chitosan in a 90 wt% acetic acid aqueous solution at room temperature. A 10 wt% PVA solution was prepared by dissolution of PVA in distilled water at 90 °C with vigorous stirring for 4 h. Then, the chitosan solution was mixed with the PVA solution at PVA:chitosan = 10:90 wt%. Besides, some other additives were also added into the above electrospinning solution, such as $CaCO_3$, $CaCl_2$ (i.e., $CaCO_3$:chitosan = 1:100 wt% and $CaCl_2$:chitosan = 1:100 wt%) to create the crystallization site.

The electrospinning experiments were performed at room temperature. The above solutions were placed into a plastic syringe (5 mL) with a metal capillary, that was, a hypodermic needle with flat-filed tip. The positive electrode of a high voltage power supply was connected to a metal capillary. An aluminum foil was used as the collector. The processing parameters of electrospinning were fixed as voltage 25 kV, feeding rate 1.0 mL/h, distance between needle tip and collector 15 cm, needle inner diameter 0.57 mm, humidity 25–45%. The prepared nanofibrous membranes were put on the top of 50 wt% glutaraldehyde aqueous solution and cross-linked by vapor of glutaraldehyde for 2 h at 25 °C. Finally, the electrospinning membranes were dried in vacuum at 40 °C overnight to remove the solvent.

The viscosity and conductivity of the chitosan/PVA blend solutions were measured by a rotational viscometer (NDJ-79, Shanghai Jichang Geology Instrument Co., Shanghai, China) and electric conductivity meter (DDB-6200, Shanghai Rex Xinjing Instrument Co., Shanghai, China), respectively.

2.3. Mineralization of nanofibrous membrane

Supersaturated solutions for crystal growth experiments were set up as following: a 100 mL beaker containing 5 mmol calcium chloride ($CaCl_2$) powder was placed into another 250 mL beaker which contain 5 mmol sodium carbonate (Na_2CO_3) powder, then deionized water was poured into inner and outer beaker until the liquid level just covered the top of inner beaker, the membrane was put on the top of inner beaker, so a $CaCO_3$ crystals could slowly deposit and grow on the membrane via diffusion of Ca^{2+} and CO_3^{2-}. The system was kept at 25 °C. The product membrane was taken out from the solution at different time intervals, then washed thoroughly with deionized water and dried in a vacuum to give the corresponding $CaCO_3$/chitosan/PVA composite product, which was negative for the chlorine test with $AgNO_3$.

The control crystallization experiment of different molar ratio of $CaCl_2$ and Na_2CO_3 (1:1, 1:2, and 2:1) without any additives and $CaCl_2$ and Na_2CO_3 = 1:1 with 0.01 wt% chitosan were made at the same setup.

2.4. Morphology of electrospun nano-fibers and $CaCO_3$ crystals

The morphological appearance of the as-spun fibers, $CaCO_3$ crystals was examined by scanning electron microscopy (SEM, Hitachi S-450, Hitachi Co., Tokyo, Japan). The average diameter of electrospun nano-fibers was determined by measurement of 50 single nano-fibers with the SEM image using image analysis software.

2.5. Mechanical characterization of the composite membranes

The mechanical properties of electrospinning fibers membranes were determined with a universal material testing machine (INSTRON1185, Instron Co., Cambridge, USA) under a cross-head speed of 10 mm/min at 23 °C. All samples were prepared in the form of dog-bone shape with straight flange dimensions of 20 mm × 5 mm. At least three repeated samples were tested for each type of electrospinning fibrous membranes.

2.6. Structure analysis of the composite membranes

FTIR spectra were obtained by a FTIR Spectrometer (Nicolet 5700, Thermo Electron Corporation, Boston, USA) using KBr pellets. The crystal phases of the obtained precipitates were identified by a X-ray diffraction (XRD, D/max-RB, Rigaku Co., Tokyo, Japan) using Ni-filtered Cu-$K\alpha$ radiation (λ = 1.5406 Å).

2.7. Characterization of biocompatibility in vitro

Viability of cells was determined by SEM (Zhou et al., 2008). The cross-linked nanofibrous mats were fixed on glass cover slips using copper tapes. The samples were then sterilized and extensively washed three times with sterile PBS prior to transfer to individual 24-well tissue culture plates. Aliquots (1 mL) of mouse fibroblasts (L929) suspension with 1.5×10^4 cell/mL were seeded on the sample membranes. After 48 h of culture, cellular constructs were harvested, rinsed twice with PBS to remove nonadherent cells, and subsequently fixed with 3.0% glutaraldehyde at 4 °C for 4 h. After that, the samples were dehydrated through a series of graded ethanol solutions and air-dried overnight. Dry samples were sputtered with gold for observation of cell morphology on the surface of the scaffolds by a JSM-5600LV SEM.

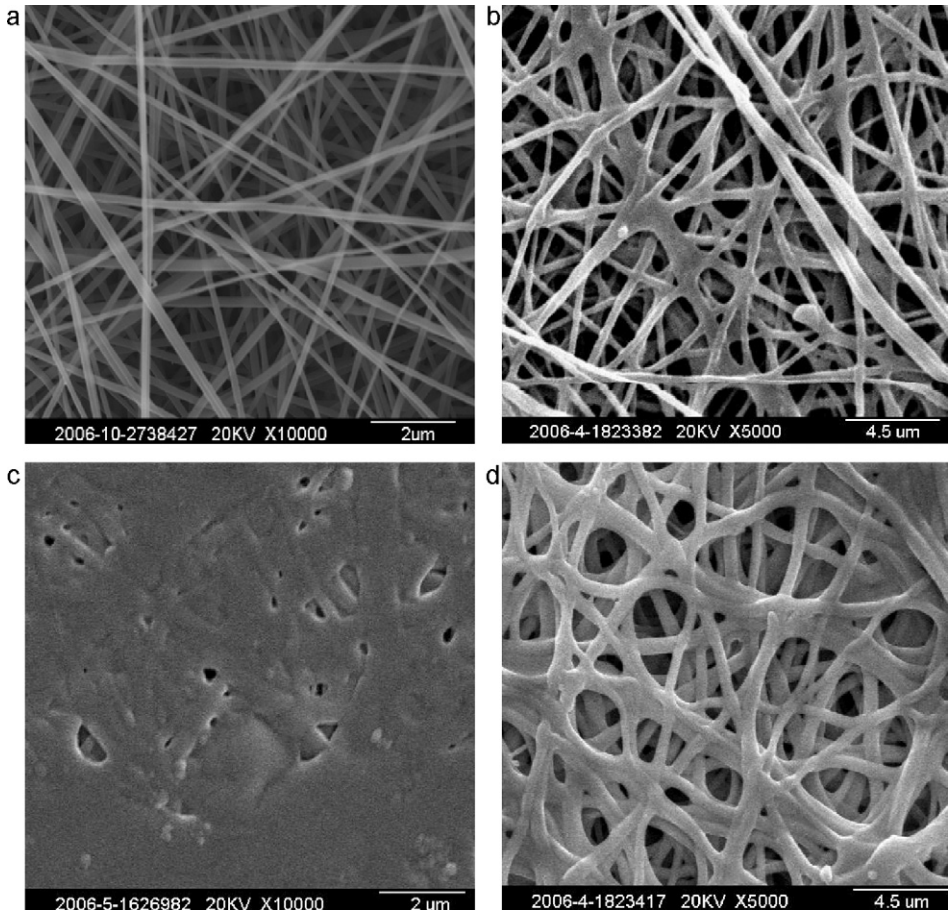

Fig. 1. SEM photographs of nanofibrous membranes. (a) PVA:chitosan = 10:90 wt% nanofibers. (b) Chitosan/PVA/$CaCO_3$ 90:10:1 wt% nanofibers. (c) Chitosan/PVA/$CaCO_3$ 90:10:1 wt% nanofibers after immersion for 1 day in supersaturated $CaCO_3$ solution. (d) Glutaraldehyde cross-linked chitosan/PVA/$CaCO_3$ (1 wt%) composite nanofibers after immersion for 1 day in supersaturated $CaCO_3$ solution.

3. Results and discussion

3.1. Morphology of electrospun nanofibers

In references Zhen, Nie, Sun, Guo, and Yang (2007) and Zhou, Yang, and Nie (2006), we showed that the chitosan acetic acid aqueous alone could not be electrospun, adding PVA to the solutions enabled fiber formation, and the higher the ratio of PVA, the higher tensile strength and elongation at break for chitosan/PVA nanofibers. In the process of electrospinning, the viscosity and conductivity of polymer solution determined by polymer concentration and additives have important influence on the morphology of nanofibers.

As mineralization membranes scaffold require mechanical stability, formation of beaded fibers should be avoided. The fine fiber morphology (see Fig. 1(a)) was achieved with chitosan 7 wt% and chitosan/PVA = 90/10 wt%, and the average fiber diameter was 200 nm. Chitosan composite nanofibers which contain 1 wt% $CaCO_3$ nano-particles were fabricated (Fig. 1(b)). But the average diameter of chitosan/PVA/$CaCO_3$ (1 wt%) fibers was increased clearly to about, and it was about 500 nm. Generally, the increase of viscosity and the decrease of conductivity of the electrospinning solution would all lead to decrease of diameter of fibers (Zhou et al., 2008). The viscosity and the conductivity increased visibly upon the addition of $CaCO_3$ nanoparticles to chitosan solution (viscosity increased from 240 mPa s to 546 mPa s and conductivity increase from 1250 $\mu s\,cm^{-1}$ to 2960 $\mu s\,cm^{-1}$ when adding 1 wt% $CaCO_3$), The two factors which have opposite effects on the diameter of fibers, perhaps the viscosity played the leading role, leaded the increase of diameters of CA/PVA/$CaCO_3$ (1 wt%) composite nanofibers. In addition, the nanofibrous membranes with small amount of $CaCO_3$ particles (chitosan:$CaCO_3$ = 100:1 wt%) had slightly lower tensile strength (2.28 MPa) then this without $CaCO_3$ (2.43 MPa).

It is well known that PVA and chitosan membrane has a high swelling in water, the chitosan/PVA nanofibrous membrane would lost its initials structure and mechanical strength after immersion in water for 1 day, as shown in Fig. 1(c). So that, it was necessary for chitosan/PVA nanofibrous membrane to crosslink, and crosslinker glutaraldehyde could improve mainly water resistance by introducing stable covalent bonds between the reactive side groups presents in chitosan and PVA chains (Fig. 1(d)). These cross-linked membranes were chosen to be mineralization matrix.

3.2. Mineralization of nanofibrous membranes

Calcification occurs when Ca^{2+} and CO_3^{2-} accumulate in concentrations that exceed their solubility within an organic matrix. After being immersed in the supersaturated $CaCO_3$ solution for 10 days, each calcificated chitosan/PVA membrane was a white sheet and kept its original shapes (as shown in Fig. 2(a)) even after drying because of solid $CaCO_3$ immobilized in the matrices. No chlorine was detected in both the products on the matrix surface and within the matrices, resulting in the slow liberation of $CaCl_2$ in aqueous Na_2CO_3 solution. $CaCO_3$ crystals with a rhombohedral morphology grow obviously as time goes on (Fig. 2(b) and (d)), the crystals were not only on the surface of the membrane but also in the inside of the membrane (Fig. 2(c)). Meanwhile, this result was proved as exam-

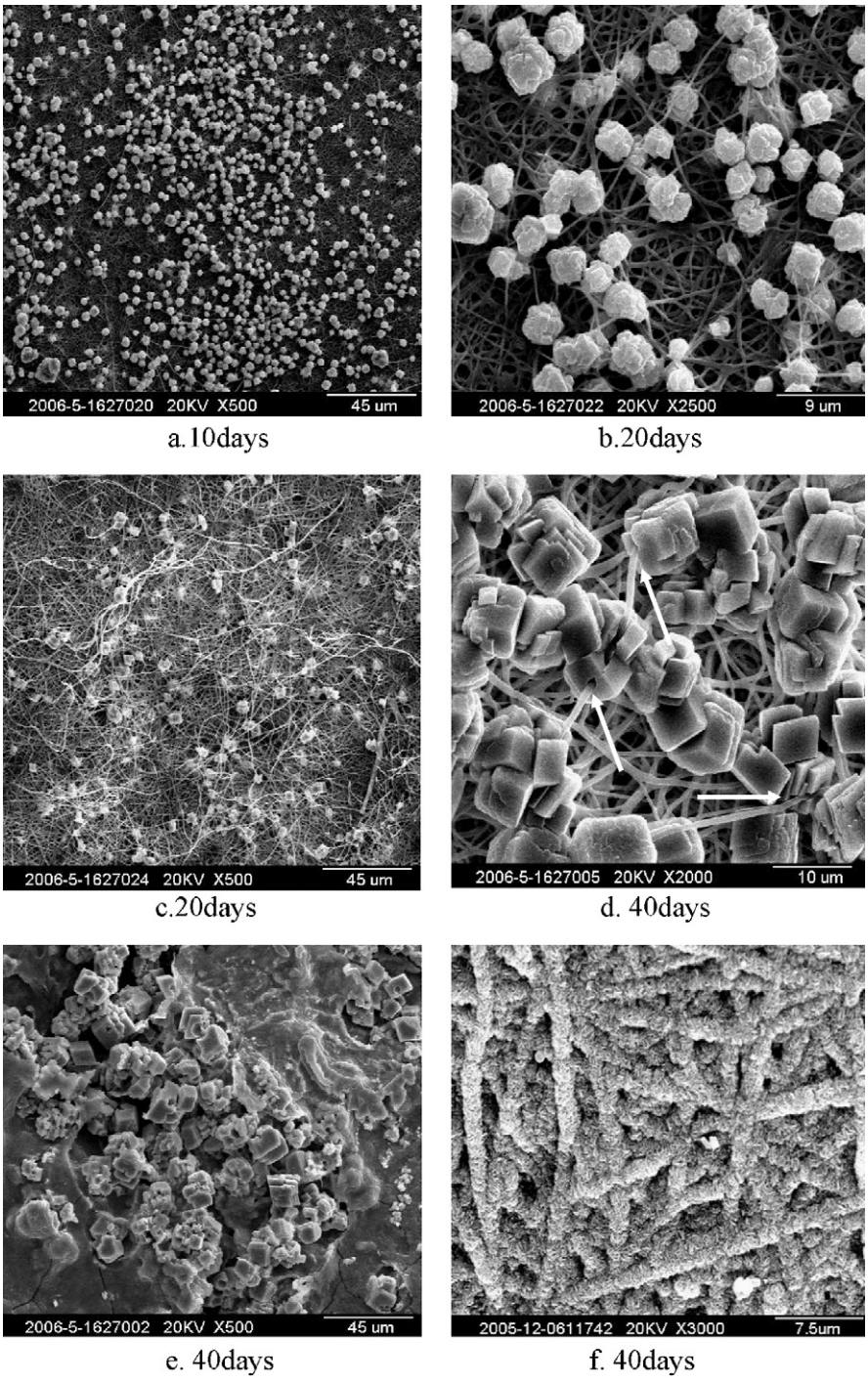

Fig. 2. SEM photographs of composite nanofibrous membrane after mineralization for different time. (a)–(e): Chitosan/PVA/$CaCO_3$ (1 wt%) membrane. f: Chitosan/PVA/$CaCl_2$ (1 wt%) membrane (c) was longitudinal section, and others were surface of membrane.

ined by IR absorptions. The formed crystals appeared in particles, which interlaced with the chitosan/PVA fibers (Fig. 2(d) as shown by the arrows). Especially, relative to chitosan/PVA/$CaCO_3$ membrane, many smaller crystal of $CaCO_3$ consecutively grown on the surface of matrix chitosan/PVA/$CaCl_2$ fibers (Fig. 2(f)). The reason deduced this results may be as follows: in the process of preparation electrospinning solution, added less than 1 wt% $CaCl_2$ to the chitosan solution, the solution still kept homogeneous, but chitosan would separate out from the solution when $CaCl_2$ more than 1 wt%, was likely to complex interaction between chitosan and Ca^{2+}. By comparison, added 1 wt% $CaCO_3$ to the chitosan solution, it inhibits the crystallization of $CaCO_3$ leads to a local high concentration inorganic ions promoted the polycrystal nucleation and the growth of $CaCO_3$ unequally. This fact indicated that the disperse degree of Ca^{2+} in the electrospinning solution influenced on the formation and polymorphs of the $CaCO_3$ crystals.

In addition, because of swilling and dissolution of chitosan and PVA, the nanofibrous structure disappeared when the non-crosslinked chitosan/PVA nanofibrous membrane immersed in the solution (Fig. 2(e)).

In nature, $CaCO_3$ has three crystal phases: calcite, vaterite, aragonite. The most commonly formed of $CaCO_3$ in biological organisms

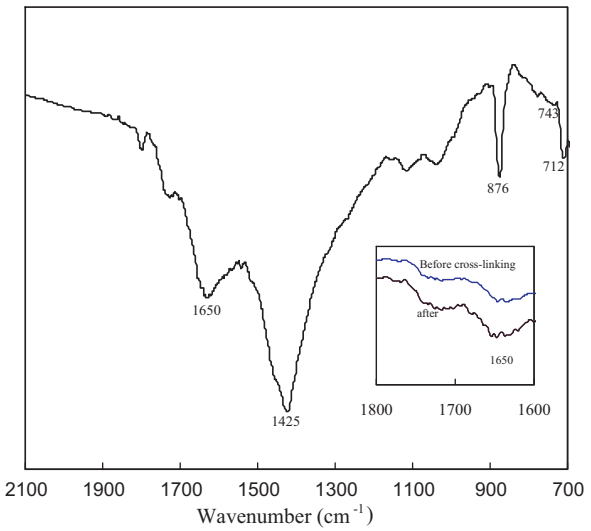

Fig. 3. FTIR spectrum of the mineralizated $CaCO_3$/PVA/$CaCl_2$ composite membranes.

are calcite and aragonite, vaterite is an unstable polymorphs and it is converted into the most thermodynamically stable calcite rapidly (Roque, Molera, & Vendrell-Saz, 2004; Weiner & Addadi, 1997).

IR adsorption bands (1425, 876, 745 and 712 cm^{-1} corresponding to CO_3^{2-}) of the crystalline polymorphs (calcite and vaterite, Xu, Han, & Cho, 2004) are clearly visible in the FTIR spectrum of the mineralizated chitosan/PVA/$CaCl_2$ composite membranes (Fig. 3). The results were in accordance with the X-ray diffraction result (Fig. 4), which confirms the presence of both calcite and vaterite phases within the final membrane. The band at 1650 cm^{-1} corresponded to amide I band of chitosan.

To further characterize the crystal structure of the deposited $CaCO_3$ on the chitosan/PVA membrane, X-ray diffraction (XRD) analysis was performed. The result indicated that the mineralized chitosan/PVA/$CaCl_2$ (1 wt%) fibrous membranes consisted of mostly calcite with a small amount of vaterite.

The XRD pattern of the $CaCO_3$ crystals in supersaturate solution containing chitosan showed in Fig. 4(b), peaks at $2\theta = 29.5^\circ$, 47.6° and 48.6° for calcite and at $2\theta = 23.2^\circ$, 27.3°, 33.2°, 36.1°, 39.5° and 43.3° for vaterite. The mineralized fibrous membranes chitosan/PVA/$CaCl_2$ (1 wt%) showed the peaks expected of a crystalline material and peaks located in the same position as $CaCO_3$, as shown in Fig. 4(a), which mainly showed the feature of calcite, meanwhile, with small amount vaterite (Takashi, Takuo, Takahiro, Taku, & Makoto, 1998). A broad peak at $2\theta = 10–25^\circ$ came from chitosan and PVA.

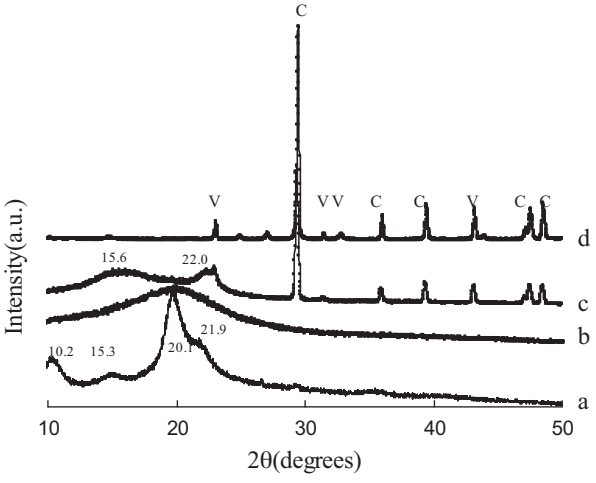

Fig. 4. XRD patterns of formed $CaCO_3$ crystals on chitosan/PVA/$CaCl_2$ (1 wt%) fibrous membranes (a) and $CaCO_3$ crystals formed in solution containing chitosan (b) (c: calcite; v: vaterite).

3.3. Effect of the composition of mineralization solution on $CaCO_3$ crystal structure

In order to reveal the interaction between $CaCO_3$ crystals and polymer scaffold, and impact of ions in the solution, the effect of molar ratio of $CaCl_2$ and Na_2CO_3 in mineralization solution on the morphology of $CaCO_3$ crystal was studied (Fig. 5a–c). The effect of polyelectrolyte chitosan on the morphology of $CaCO_3$ was investigated as well (Fig. 5d).

In the case of different ratio of $CaCl_2$ and Na_2CO_3 without any additives, a lot of $CaCO_3$ crystals occurred in the solution, and the shape and dimension of these crystals were varying. However, it was in calcite form confirmed by X-ray analysis. The ratio of $CaCl_2$ and Na_2CO_3 in the solution did not have much effect on the crystal morphology.

The SEM micrographs of the $CaCO_3$ crystals collected in the presence of chitosan in the incubation solution showed that the $CaCO_3$ crystals were mostly in calcite form. However, the crystals showed abnormal shape, because of adsorbed polymer on nanocrystal surfaces may be lead to the difference of growth rate in each crystal face of $CaCO_3$ polymorph. The aggregation of nanocrystals led to various shapes of the final $CaCO_3$ crystal.

3.4. Mechanism

Similar to biomineralization, heterogeneous nucleation of $CaCO_3$ crystal is crucial for its successful growth on chitosan/PVA membrane surface, because only heterogeneous nucleation can produce strong bonds at the interface between the polymer phase and mineral crystals. Adding $CaCO_3$ or $CaCl_2$ to chitosan/PVA solution prior to electrospinning is a good method to promote heterogeneous nucleation.

Several factors could influence mineral nucleation and crystal growth on a polymer film, such as the degree of saturation of a supersaturated solution and the surface charges on a polymer film. It is crucial for successful mimetic synthesis that only heterogeneous nucleation be promoted on the polymer film and that homogeneous nucleation be suppressed in the mother liquid. Saturation of the mother solution favours homogeneous nucleation from solution. On the other hand, one key factor for successfully mineralization on organic polymer substrates is to increase the density of charges or polarity on the substrate surface (Zhang & Gonsalves, 1998). In this work, the electrospinning solution was prepared by dissolution chitosan in a concentrated acetic acid, and a lot of amino group of chitosan were protonized, and the density of charges on the electrospinning membranes increased.

Besides, in order to provide nucleated forerunner ion of $CaCO_3$ crystals inside or on the surface of fiber, a small amount of $CaCl_2$ or $CaCO_3$ were added to the electrospinning solutions. The radius of Ca^{2+} was only 0.174 nm, and average diameter of the electrospinning fibers of chitosan was 100–200 nm, so that, Ca^{2+} could penetrated into the inside of swelling fibers, and also on the surface of fiber. So the crystals could grow both ways.

The possible mechanism of $CaCO_3$ particle growth on chitosan/PVA nanofibrous membrane derived from the XRD, SEM, and FT-IR results could be elucidated as follows: first, calcium ions were dissolved into polymer matrixes solution and nucleation occurred throughout the chitosan/PVA nanofibers, followed by the crystal growth into vaterite particles until they were closed together with

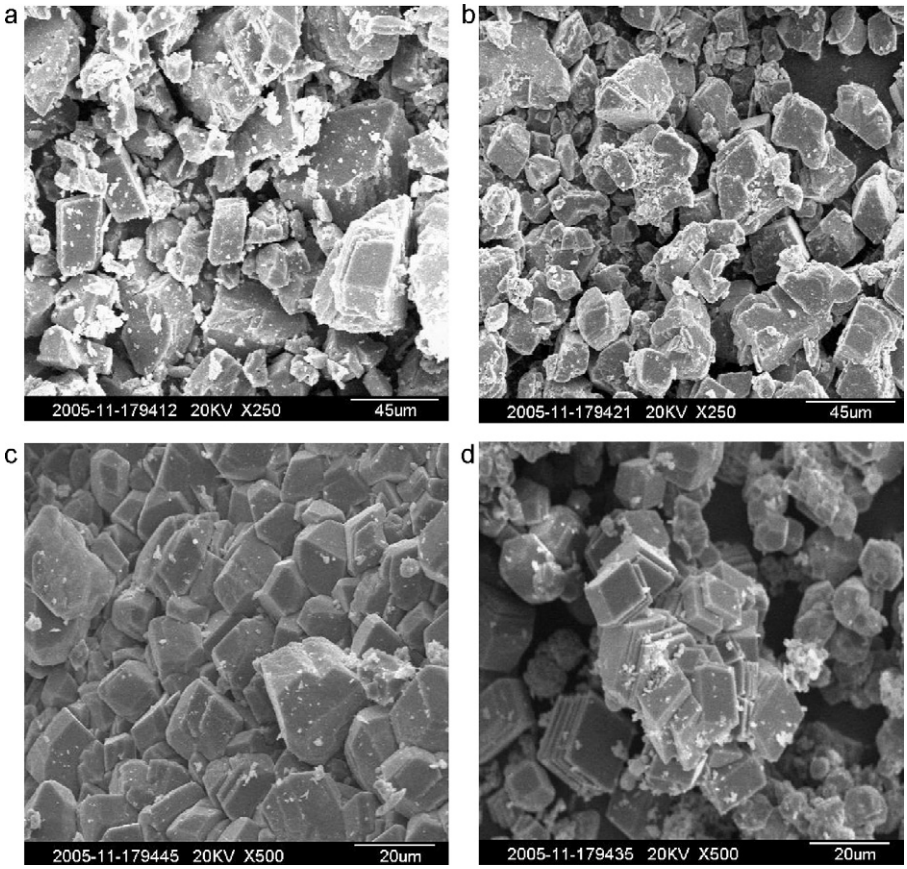

Fig. 5. SEM photographs of a large-area $CaCO_3$ crystals formed in the supersaturated $CaCO_3$ solution made of molar ratio of $CaCl_2$:Na_2CO_3 (a) 1:2, (b) 1:1, (c) 2:1, and (d) 1:1, 0.01 wt% chitosan was added to the mineralization solution.

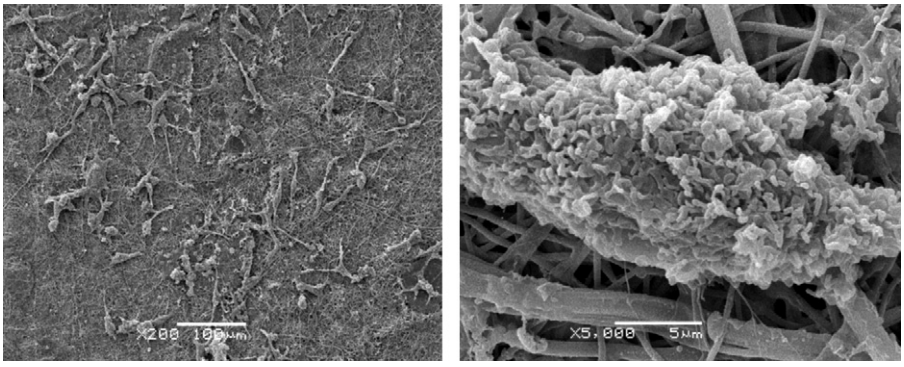

Fig. 6. SEM images of mouse fibroblasts grown on $CaCO_3$–chitosan/PVA fibrous membranes after 2 day culture.

neighboring particles, and finally formed most stable calcite crystal form. The composite structure was not a simple formation of a $CaCO_3$ layer was on the polymer nanofibers, but $CaCO_3$ particles dispersed in polymer matrixes.

3.5. Biocompatibility

To examine the biocompatibility of composite scaffold, an indirect cytotoxicity test was conducted by using mouse fibroblasts (L929) cells. Even though we were interested in using the obtained mineralized mats as potential bone scaffolds, it was mandatory to test the materials with L929 just to comply with the ISO10993-5 standard test method. The electron micrograph of the cells grown on the scaffold fiber for 48 h is shown in Fig. 6. The cells were observed to grow normally on the composite fibrous mesh.

4. Conclusions

In this study, a new type of biocomposite membranes was designed by mineralization method of chitosan/PVA/Ca^{2+} electrospun nanofibers in the supersaturated $CaCO_3$ solution. The structure of membranes and crystal type of $CaCO_3$ was examined by FTIR, X-ray and SEM observation. The composite structure suggested that the calcite $CaCO_3$ crystals grew both on the surface and in the inner of the membrane. It is possible process can be briefly summarized as follows: first, calcium ions were dissolved into polymer matrixes solution and nucleation occurred throughout the chitosan/PVA nanofibers, followed by the crystal growth into vaterite particles until they were closed together with neighboring particles, and finally formed most stable calcite crystal form. MTT test and SEM imaging indicated

that the biocompatibility of composite membrane was well for bioapplication.

In order to apply this mineralization to field of bone restoration, further study of osteoblast function, hydrolysis behavior of chitosan/PVA nanofibrous membranes and a bone healing activity is necessary. However, the present study showed the potential of chitosan/PVA/$CaCO_3$ composite nanofibrous for induction $CaCO_3$ crystal in vitro environment, the inorganic/organic composite reported here may provide new biomimetic materials with specific mechanical and biological properties.

Acknowledgment

The author would like to thank the National Natural Science Foundation of China (50803004) and the Natural Science Foundation of Beijing City (2112033) for its financial support.

References

Doshi, J., & Reneker, D. H. (1995). Electrospinning: A whipping fluid jet generates submicron polymer fibers. *Journal of Electrostatics*, *2*(3), 151–160.

Egan, T. J., Mavuso, W. W., & Ncokazi, K. K. (2001). The mechanism of β-hematin formation in acetate solution. Parallels between hemozoin formation and biomineralization processes. *Biochemistry*, *1*, 204–213.

Ehrlich, H., Krajewska, B., Hanke, T., Born, R., Heinemann, S., Knieb, C., et al. (2006). Chitosan membrane as a template for hydroxyapatite crystal growth in a model dual membrane diffusion system. *Journal of Membrane Science*, *1–2*, 124–128.

Gao, Z., He, L. S., Chen, F. L., & Yi, F. Z. (2003). The development in the study of scaffold materials for bone tissue engineering. *International Journal of Biomedical Engineering*, *5*, 223–226.

Gooday, G. W., Prosser, J. I., illman, K., & Cross, M. G. (1991). Mineralization of chitin in an estuarine sediment: The importance of the chitosan pathway. *Biochemical Systematics and Ecology*, *19*(5–6), 395–400.

Grassmann, O., Muller, G., & Lobmann, P. (2002). Organic–inorganic hybrid structure of calcite crystalline assemblies grown in a gelatin hydrogel matrix: Relevance to biomineralization. *Chemistry of Materials*, *14*, 4530–4535.

He, G., Gajjeraman, S., Schultz, D., Cookson, D., Qin, C., Butler, W. T., et al. (2005). Spatially and temporally controlled biomineralization is facilitated by interaction between self-assembled dentin matrix protein 1 and calcium phosphate nuclei in solution. *Biochemistry*, *49*, 16140–16148.

Hirano, S., Inui, H., & Yamamoto, K. (1995). The mineralization of CO3–2 ions in crab shells, and their mimetic composite materials. *Energy Conversion and Management*, *6–9*, 783–786.

Hirano, S., Yamamoto, K., & Inui, H. (1997). Calcium chloride as a biomimetic intermediate for the mineralization of carbonate ions of water as calcium carbonate in gelatinous matrices of chitosan and chitin. *Energy Conversion and Management*, *1*, 517–521.

Ho, M. H., Wang, D. M., Hsieh, H. J., Liu, H. C., Hsien, T. Y., Lai, J. Y., et al. (2005). Preparation and characterization of RGD-immobilized chitosan scaffolds. *Biomaterials*, *16*, 3197–3206.

Liang, P., Zhao, Y., Shen, Q., Wang, D. J., & Xu, D. F. (2004). The effect of carboxymethyl chitosan on the precipitation of calcium carbonate. *Journal of Crystal Growth*, *261*, 571–576.

Mann, S. (2001). *Biomineralization: Principles and Concepts in Bioinorganic Materials Chemistry*. New York: Oxford University Press., pp. 20–80.

Muzzarelli, R. A. A. (2009). Chitins and chitosans for the repair of wounded skin, nerve, cartilage and bone. *Carbohydrate Polymers*, *76*, 167–182.

Muzzarelli, R. A. A. (2011). Chitosan composites with inorganics, morphogenetic proteins and stem cells, for bone regeneration. *Carbohydrate Polymers*, doi:10.1016/j.carbpol.2010.10.044

Neira-Carrillo, A., Yazdani-Pedram, M., Retuert, J., Diaz-Dosque, M., Gallois, S., & Arias, J. L. (2005). Selective crystallization of calcium salts by poly(acrylate)-grafted chitosan. *Journal of Colloid and Interface Science*, *286*(1), 134–141.

Nissan, B. B. (2003). *Natural bioceramics*: From coral to bone and beyond. *Current Opinion in Solid State and Materials Science*, *7*, 283–288.

Osamu, S. (2005). Interface of synthetic inorganic biomaterials and bone regeneration. *International Congress Series*, *1284*, 274–283.

Piattelli, A., Podda, G., & Scarano, A. (1997). Clinical and histological results in alveolar ridge enlargement using coralline calcium carbonate. *Biomaterials*, *18*, 623–627.

Reneker, D. H., & Chun, I. (1996). Nanometre diameter fibres of polymer, produced by electrospinning. *Nanotechnology*, *3*, 216–223.

Rhoads, A, Beyenal, H., Lewandowski, & Environ, Z. (2005). Microbial fuel cell using anaerobic respiration as an anodic reaction and biomineralized manganese as a cathodic reactant. *Science and Technology*, *12*, 4666–4671.

Roque, J., Molera, J., & Vendrell-Saz, M. (2004). Crystal size distributions of induced calcium carbonate crystals in polyaspartic acid and Mytilus edulis acidic organic proteins aqueous solutions. *Journal of Crystal Growth*, *262*, 543–553.

Storrie, H., & Stupp, S. I. (2005). Cellular response to zinc-containing organoapatite: An in vitro study of proliferation, alkaline phosphatase activity and biomineralization. *Biomaterials*, *27*, 5492–5499.

Takashi, K., Takuo, S., Takahiro, A., Taku, I., & Makoto, K. (1998). Effects of macromolecules on the crystallization of $CaCO_3$ the formation of organic/inorganic composites. *Supermolecular Science*, *5*, 411–415.

Walsh, W. R., Chapman-Sheath, P. J., Cain, S., Debes, J., Bruce, W. J. M., Svehla, M. J., et al. (2003). A resorbable porous ceramic composite bone graft substitute in a rabbit metaphyseal defect model. *Journal of Orthopaedic Research*, *21*, 655–661.

Weiner, S., & Addadi, L. (1997). Design strategies in mineralized biological material. *Journal of Materials Chemistry*, *5*, 689–702.

Xu, X. R., Han, J. T., & Cho, K. (2004). Formation of amorphous calcium carbonate thin films and their role in biomineralization. *Chemistry of Materials*, *16*, 1740–1746.

Yang, D. Z., Jin, Y., Zhou, Y. S., Chen, X. M., Lu, F. M., & Nie, J. (2008). In situ mineralization of hydroxyapatite on electrospun chitosan-based nanofibrous scaffolds. *Macromolecular Bioscience*, *8*, 239–246.

Zhang, Q. Y., Chen, J. Y., Feng, J. M., Cao, Y., Deng, C. L., & Zhang, X. D. (2003). Dissolution and mineralization behaviors of HA coatings. *Biomaterials*, *26*, 4741–4748.

Zhang, S., & Gonsalves, K. E. (1998). Influence of the chitosan surface profile on the nucleation and growth of calcium carbonate films. *Langmuir*, *23*, 6761–6766.

Zhang, G., Wang, D., Gu, Z. Z., Hartmann, J., & Mohwald, H. (2005). Two-dimensional non-close-packing arrays derived from self-assembly of biomineralized hydrogel spheres and their patterning applications. *Chemistry of Materials*, *21*, 5268–5274.

Zhen, H. P., Nie, J., Sun, J. F., Guo, S., & Yang, D. Z. (2007). Kinetics studies on polymerization of diethyldiallylammonium chloride and its copolymerization with acrylamide and acrylic acid. *Acta Polymerica Sinica*, *2*, 183–187.

Zhou, Y. S., Yang, D. Z., Chen, X. M., Xu, Q., Lu, F. M., & Nie, J. (2008). Electrospun water-soluble carboxyethyl chitosan/poly(vinyl alcohol) nanofibrous membrane as potential wound dressing for skin regeneration. *Biomacromolecules*, *9*, 349–354.

Zhou, Y. S., Yang, D. Z., & Nie, J. (2006). Electrospinning of chitosan/poly(vinyl alcohol)/acrylic acid aqueous solutions. *Journal of Applied Polymer Science*, *102*, 5692–5697.